Characterization of the Fast and Slow Reversible Components of Non-Photochemical Quenching in Isolated Pea Thylakoids by Picosecond Time-Resolved Chlorophyll Fluorescence Analysis†

Michael Richter*

Institut für Allgemeine Botanik, Johannes Gutenberg-Universität, Saarstrasse 21, D-55099 Mainz, Germany

Reimund Goss

Institut für Botanik, Johannisallee 21-23, Universität Leipzig, D-04103 Leipzig, Germany

Birgit Wagner

Institut für Molekulare Biotechnologie, Beutenbergstrasse 11, D-07745 Jena, Germany

Alfred R. Holzwarth

Max-Planck-Institut für Strahlenchemie, Stiftstrasse 34-36, D-45470 Mülheim an der Ruhr, Germany

Received December 22, 1998; Revised Manuscript Received July 13, 1999

ABSTRACT: The fast and slow reversible components of non-photochemical chlorophyll fluorescence quenching commonly assigned to the qE and the qI mechanism have been studied in isolated pea thylakoids which were prepared from leaves after a moderate photoinhibitory treatment. Chlorophyll fluorescence decays were measured at picosecond resolution and analyzed on the basis of the heterogeneous exciton/radical pair equilibrium model. Our results show that the fast reversible non-photochemical quenching is completely assigned to the PS II antenna and is related to zeaxanthin. The slow reversible qI type quenching is located at the PS II reaction center and involves enhanced nonradiative decay of the primary charge separated state to its ground state and/or triplet excited state. Apart from its independence from the proton gradient, the qI quenching shows striking similarities to a particular form of qE quenching which is also located at the PS II reaction center and has resently been resolved in isolated thylakoids from dark-adapted leaves [Wagner, B., et al. (1996) *J. Photochem. Photobiol., B 36,* 339−350]. Our data suggest that during exposure to the supersaturating light the reaction center qE component was replaced by qI quenching. This qE to qI transition is supposed to be part of the mechanism of the long-term downregulation of PS II during photoinhibition. It is also evident that under the conditions used in our study zeaxanthin-dependent antenna quenching is not involved in the slow reversible downregulation of PS II but that it retains its dependence on the proton gradient during exposure to strong light.

It is a basic property of the photosynthetic apparatus of all plants that it cannot use the full range of naturally occurring solar irradiance at high quantum yields in photosynthetic production. PS II[1] which is a potential target of adverse effects of strong light is protected by flexible mechanisms for a harmless thermal dissipation of light absorbed in excess. In the photochemically closed PS II, where only heat and chlorophyll fluorescence compete for the excitation energy, thermal dissipation is reflected in the so-called non-photochemical quenching (NPQ) of chlorophyll fluorescence. As indicated by the kinetics of dark relaxation, different types of NPQ can be distinguished (*1*) which have been reviewed by Krause and Weis (*2*). Under excessive illumination, one major component of NPQ is the so-called high-energy-state quenching (qE) which is linked to the light-induced formation of a ΔpH gradient across the thylakoid membrane (*3*) and thus is normally reversed soon upon return to dark. It has been proposed that qE itself is composed of two different quenching mechanisms both of which depend on the ΔpH, but only one being related to zeaxanthin (*4*). This heterogeneity in qE has recently been confirmed in a chlorophyll fluorescence lifetime study with isolated pea thylakoids which was based on the exciton/radical pair equilibrium model [*5*; see also Goss et al. (*6*)]. With this approach, it was possible to distinguish between zeaxanthin- and ΔpH-dependent antenna quenching and purely ΔpH-

† This work was supported by the Deutsche Forschungsgemeinschaft (Wi 243/19-2) and Sonderforschungsbereich 189, Heinrich-Heine-Universität, Düsseldorf, and Max-Planck-Institut für Strahlenchemie, Mülheim.

[1] Abbreviations: P or P-680, primary donor of PS II; DAS, decay-associated fluorescence spectrum; DCMU, 3-(3,4-dichlorphenyl)-1,1-dimethylurea; DTT, dithiothreitol; F_o, F_v, and F_m, initial, variable, and maximal chlorophyll fluorescence yields, respectively; I, pheophytin (primary electron acceptor of PS II); LHC II, light-harvesting complex II; NPQ, non-photochemical chlorophyll fluorescence quenching; PS II, photosystem II; PFD, photon flux density; Q_A, primary electron-accepting plastoquinone of PS II; Q_B, secondary electron-accepting plastoquinone of PS II; qE and qI, fast and slow reversible non-photochemical quenching, respectively.

10.1021/bi983009a CCC: $18.00
Published on Web 09/03/1999

dependent quenching at the reaction center in the closed PS II. According to the exciton/radical pair equilibrium model, the reaction center quenching was caused by nonradiative recombination of the charge separated state of the primary donor P-680 and the primary acceptor pheophytin (P^+I^-) to the ground state (PI). The extents of both types of qE quenching were shown to be rapidly reduced upon uncoupling of the respective thylakoids.

With increasing durations and intensities of the strong light treatment on leaves, usually a slowly relaxing second component of NPQ emerges. It has been termed "photoinhibitory quenching" (qI) because it occurrs during photoinhibition. There is, however, growing evidence that qI does not simply reflect damage to PS II but may, instead, represent a mechanism of long-term downregulation of PS II (*7*) which would partly replace the fast reversible qE mechanism under conditions of prolonged strong light exposure (*8*). The site of downregulation was supposed to be the reaction center (*8*, *9*).

In contrast, several attempts were made to show that qI quenching induced by strong light is related to the PS II antenna through the maintenance of high zeaxanthin contents in the dark (*10*−*12*), stable protonations of the LHC II (*13*), or the maintenance of a proton gradient in the dark by ATP hydrolysis (*14*).

In this work, fast and slow reversible non-photochemical quenching of chlorophyll fluorescence as well as possible relations of both to zeaxanthin were studied in isolated thylakoids from moderately photoinhibited leaves. Picosecond time-resolved chlorophyll fluorescence decay kinetics were measured and analyzed in terms of the exciton/radical pair equilibrium model by Schatz et al. (*15*).

MATERIALS AND METHODS

Samples. Pea plants (*Pisum sativum* var. Kleine Rheinländerin) were cultivated in a growth chamber with a 16 h−8 h light−dark regime at a PFD of 100 μmol m^{-2} s^{-1} of photosynthetically active radiation (PAR). The 14−16-day-old plants were harvested during growth light.

The moderate photoinhibitory light treatment consisted of an illumination of detached pea leaves at a PFD of 750 μmol m^{-2} s^{-1} (PAR) for 20 min in a normal atmosphere. Desiccation of the plant material was prevented by floating the pea leaves on a water surface. To avoid possible side effects of heat radiation, the photoinhibitory light was filtered through 8 cm of water, and the leaf chamber temperature was held constant at 20 °C. Control leaves were kept in the dark under otherwise identical conditions.

Chloroplasts from pea leaves were prepared according to the method of Chow and Anderson (*16*) with minor modifications. In a second preparatory step, the chloroplasts were osmotically shocked by incubation for 2 min in a medium containing 10 mM NaCl, 5 mM $MgCl_2$, and 10 mM HEPES/NaOH (pH 6.5). After a short centrifugation at 1700*g*, the thylakoids were resuspended in the isolation medium according to the method of Chow and Anderson and stored on ice.

The effects of the moderate photoinhibitory light treatment on non-photochemical energy dissipation were investigated by means of chlorophyll fluorescence measurements using isolated pea thylakoids prepared from the illuminated or dark-adapted intact leaves. The basic reaction medium for the chlorophyll fluorescence measurements was composed of 100 mM sorbitol, 10 mM NaCl, 5 mM $MgCl_2$, 1 mM EDTA, and 50 mM HEPES/NaOH (pH 7.8).

Three different conditions were chosen to differentiate between the effects of fast reversible high-energy-state quenching (qE) and slow reversible non-photochemical quenching of chlorophyll fluorescence (qI). The first condition ("light, +ΔpH" sample) included energization of isolated thylakoids from moderately photoinhibited leaves by a proton gradient established by ATP hydrolysis in the dark. We chose this way of thylakoid energization with regard to the special requirements of fluorescence measurements by single-photon timing (SPT). Care was taken that the pH gradient was stable for the appropriate sampling period, 10 min in our case. The buildup of the ΔpH gradient was induced by adding 0.3 mM ATP to the thylakoid suspensions and then activating the ATPase by a short light treatment of 3 min at 360 μmol m^{-2} s^{-1} before the fluorescence measurement. The second condition ("light, −ΔpH" sample) also included thylakoids from moderately photoinhibited leaves. In contrast to the first condition, the addition of ATP and the ATPase activating light period were omitted, making sure that these thylakoids remained in the nonenergized state throughout the fluorescence measurement. The third condition served as reference ("reference" sample). These thylakoids were prepared from dark-adapted leaves and were then kept nonenergized by omitting the ATPase activating light period and the addition of ATP. In the case of the nonenergized samples ("light, −ΔpH" and "reference"), sampling periods of the SPT measurements were prolonged to 50 min.

Determination of the Xanthophyll Pigment Composition. The concentrations of the xanthophyll cycle pigments violaxanthin, antheraxanthin, and zeaxanthin were determined using reversed phase high-performance liquid chromatography (HPLC). A baseline separation of lutein and zeaxanthin was achieved on a Zorbax ODS column (250/4.6 mm, C18, particle size of 5 μm, 20% C, Rockland Technologies) by binary gradient elution with eluents A [98:2 acetonitrile/Tris-HCl (pH 7.8)] and B (75:25 methanol/ethyl acetate) (*5*). The concentrations of the individual xanthophylls are expressed as percentages of the total xanthophyll cycle pool. Pigments were measured from thylakoids prepared from dark-adapted or moderately photoinhibited pea leaves. In addition, we measured the xanthophyll contents of the "light, +ΔpH" sample after the completion of the SPT measurements to make sure that no changes in the pigment stoichiometries had occurred due to the specific sample treatment involving a short ATPase activating light period and a subsequent dark incubation in the presence of a proton gradient.

Fluorescence Induction. Room-temperature chlorophyll fluorescence induction curves were obtained with a fluorometer with a low-intensity modulated measuring light (PAM 101, Walz, Germany). The thylakoid suspensions had a chlorophyll content of 100 mg/L. For the "light, +ΔpH" samples, the maximum fluorescence yield was monitored with application of short saturating flashes (5500 μmol m^{-2} s^{-1}) over the course of 3 min of the ATPase activating light period (360 μmol m^{-2} s^{-1}). After 3 min, DCMU (10 μM) and hydroxylammonium chloride (1 mM) were simultaneously added to close all PS II reaction centers without

further saturating flashes. The weak modulated measuring beam was now sufficient to maintain a permanent closure of PS II during the time span of 10 min corresponding to the sampling periods of the single-photon timing. In the case of the nonenergized samples ("light, $-\Delta$pH" and "reference"), closure of the reaction centers by DCMU and $HONH_3Cl$ followed immediately after the application of one saturating light flash.

Fluorescence induction measurements with the PAM fluorometer mainly served the purpose of controlling the fluorescence data obtained with the single-photon timing measurements. Under identical conditions, the changes in the maximum fluorescence yield (F_m) in PAM measurements were equal within error limits to the respective changes in count rates obtained with single-photon timing.

Fluorescence Decays. Fluorescence decays were recorded by the method of single-photon timing (SPT). For excitation, we used a synchronously pumped mode-locked and cavity-dumped dye laser system (models 375 and 455S, Spectra Physics) with an Ar^+ laser (model 171, Spectra Physics) as the pumping source. The excitation wavelength was set to 643 nm. At a repetition rate of 800 kHz, the pulse width (fwhm) was 14 ps. The sample was excited with an excitation density of 40 nJ pulse^{-1} cm^{-2}.

The fluorescence was dispersed by a spectrograph (HR 250, Jobin Yvon) positioned at 90° with respect to excitation. To suppress stray light, a cutoff filter (RG 665, Schott) was placed in front of the spectrograph. A multianode microchannel plate photomultiplier (R 3839 U-11, Hamamatsu) was used for detection. This special arrangement allowed for the simultaneous measurement of fluorescence at four different detection wavelengths with a spectral resolution of 8 nm/anode (fwhm). The signals of four anodes were processed with four sets of equivalent detection electronics. Each set consisted of a constant fraction discriminator (TC 454, Tennelec), a time-to-amplitude converter (TC 862, Tennelec), and an analog-to-digital converter (7423 UHS, Silena). The signals were then stored in four multichannel analyzers (TMCA, target) integrated in a personal computer. The resolution of the time-to-amplitude converter was 10 ps/channel. The system response function was measured for each anode separately and exhibited a half-width of 65−70 ps. After deconvolution of the decay curves with the system response function, a resolution of <10 ps could be achieved. Fluorescence decays were measured between 676 and 698 nm. A minimum of 23 000 counts was collected in the peak channel of the multichannel analyzer.

For SPT measurements, samples containing 10 μg of Chl/mL were pumped from a reservoir through a flow cuvette (1.5 mm × 1.5 mm × 1.5 mm) at a flow rate of 100 mL/min. The fluorescence decays of the different samples were measured with closed reaction centers (F_m). Closure of the reaction centers was achieved by addition of 1 mM $HONH_3$-Cl and 10 μM DCMU and preillumination of the sample before entering the flow cuvette. For this purpose, a glass tube with a diameter of 4 mm was inserted in the flow system and illuminated with 2.5 μmol m^{-2} s^{-1}. In the case of "light, $+\Delta$pH" samples, hydroxylammonium chloride and DCMU were added after the ATPase activating actinic light period. The sample temperature was kept constant at 15 °C. The sampling periods were limited to 10 min, which was short enough to ensure sufficient stability of the proton gradient

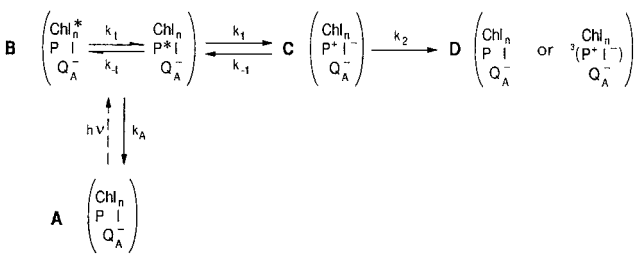

FIGURE 1: Exciton/radical pair equilibrium model for the primary processes in photosystem II according to ref *15*. The scheme represents the model of the closed photosystem II with the maximal fluorescence yield (F_m) due to a permanently reduced electron-accepting plastoquinone Q_A. State A represents PS II in the ground state which is transferred to the excited state B by light absorption. Since the model assumes trap-limited exciton decay (k_t, $k_{-t} \gg k_1$), states (Chl_n*PIQ_A^-) and (Chl_nP*IQ_A^-) are treated as one generalized excited state. The latter leads forward to the primary charge-separated state C as described by the rate constant k_1. Alternatively, radiative and nonradiative decay back to the ground state are combined in rate constant k_A. Since the stabilization of the charge separation is not possible in the closed PS II, the singlet radical pair of state C may only recombine to the excited state B as described by rate constant k_{-1} or to state D, which can be reached by the nonradiative decay back to the ground state and/or triplet excited state of the radical pair, both summarized in rate constant k_2.

during the SPT measurement. To achieve the minimum of 23 000 counts in the peak channel of the multichannel analyzer (MCA), the counts of five independent measurements, each performed with a fresh sample, were summed up. For nonenergized samples ("light, $-\Delta$pH" and "reference"), the data collection intervals were 50 min.

Data Analysis. Fluorescence decay data were first analyzed by a global lifetime analysis. In this analysis procedure, the fluorescence decay curves recorded at different wavelengths were simultaneously fitted by a sum of exponentials $[\Sigma_i a_i(\lambda) \exp(-t/\tau_i)]$. The fit quality was judged by a reduced χ^2 criterion and plots of the weighted residuals. For each lifetime component, the dependency of amplitudes a_i on detection wavelength λ is shown in decay-associated spectra (DAS).

Second, a global target analysis was performed on the basis of the exciton/radical pair equilibrium model presented by Schatz et al. (*15*) which had been used previously to successfully fit data from time-resolved fluorescence and absorption measurements (*15*, *17*, *18*), demonstrating that it is appropriate for the description of the primary kinetic processes in PS II. In this model (Figure 1), four different states of PS II designated A−D are considered. The model is characterized by four rate constants and assumes a trap-limited energy transfer. Further details of the model are given in the legend of Figure 1.

There is evidence pointing to the existence of two different populations of PS II, called PS IIα and PS IIβ (for a review, see ref *19*). They probably differ in their relative antenna size (*20*), while the evidence regarding their localization in appressed and nonappressed thylakoids is still contradictory (*21*, *22*). This heterogeneity was taken into account in the analysis using the fitting approach developed by Roelofs et al. (*23*) and resulted in eight rate constants: four for each type of PS II. Furthermore, a factor was calculated that represents the ratio of the number of absorbing chlorophyll molecules (relative antenna size) in the respective antenna types (α and β). According to the observation that PS IIα has the larger antenna size (*20*), it was attributed to the

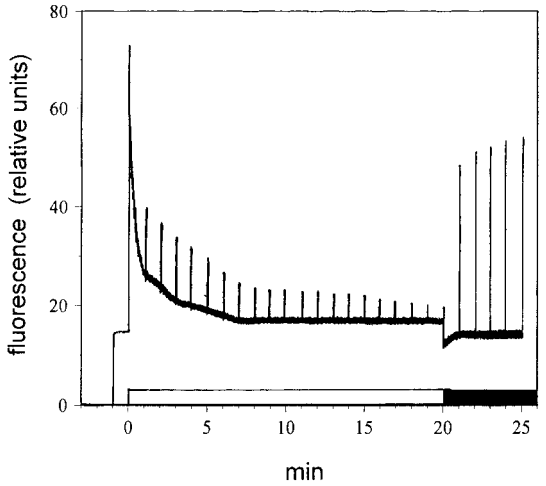

FIGURE 2: Chlorophyll fluorescence induction kinetics of pea leaves in moderate photoinhibitory light (20 min, 750 μmol m^{-2} s^{-1}). The moderate photoinhibitory treatment and the dark recovery are represented by the white and black bars at the bottom, respectively. Starting from the dark-adapted state, saturating light pulses (1 s, 5500 μmol m^{-2} s^{-1}) for the determination of the maximal fluorescence yield were supplied every minute.

majority of chlorophyll molecules. The model predicts two lifetimes for each type of PS II, and thus, the kinetic analysis yields a sum of four lifetimes for PS II.

All parameters except for the ones that are kept fixed in each case were allowed to vary freely.

RESULTS

Fluorescence Induction. With the onset of the moderate photoinhibitory light treatment, detached pea leaves developed non-photochemical chlorophyll fluorescence quenching (NPQ) as determined by the decline of the maximal yield of chlorophyll fluorescence (F_m) obtained with saturating light pulses (Figure 2). Part of the overall NPQ relaxed within the first 5 min of dark adaptation, indicating the operation of the fast reversible qE mechanism in the preceding strong light period. The fast phase of recovery of the F_m level was typically accompanied by a reduction in the extent of quenching of the dark level of chlorophyll fluorescence (F_o, Figure 2). The intensity and the duration of the strong light treatment on leaves were chosen such that the slow relaxing type of quenching (qI quenching) just started to develop. These conditions were chosen so complications in the analysis of the fluorescence decay data due to the complex changes associated with more severe photoinhibition could be avoided, e.g., the disassembly of parts of PS II (*24*). After 5 min of dark recovery of the leaves, the decrease in F_m, as compared to that of the dark-adapted state at the beginning of the strong light treatment, ranged between 20 and 25%. The slowly proceeding dark recovery from qI quenching, which can normally be observed with whole leaves, was absent at the level of the isolated thylakoids from moderately photoinhibited leaves. Thylakoids prepared immediately from the pea leaves after the strong continuous light treatment was terminated ("light, −ΔpH" sample) exhibited a constant loss in F_m of up to 26% (Figure 3). If a proton gradient from ATP hydrolysis was established across these thylakoids ("light, +ΔpH" sample), a further NPQ was added upon the existing ΔpH-independent NPQ, leading to a total decrease in F_m of about 50% (Figure 3). The closed PS II in samples

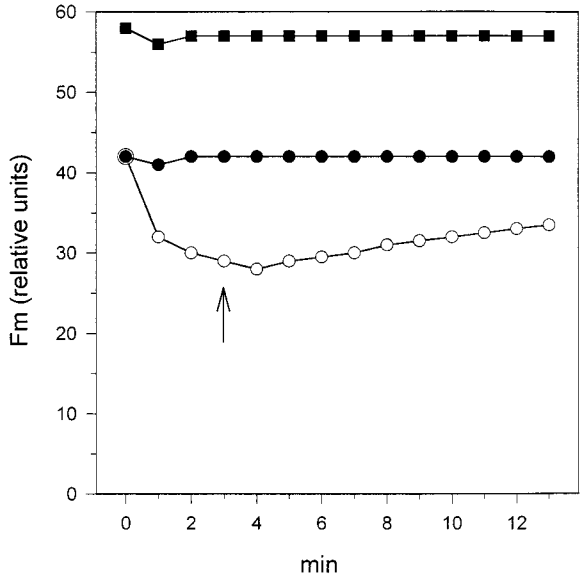

FIGURE 3: Time course of the maximal chlorophyll fluorescence yield (F_m) of pea thylakoids. The thylakoids were prepared from either dark-adapted ["reference" sample (■)] or moderately photoinhibited pea leaves ["light, −ΔpH" sample (●) and "light, +ΔpH" sample (○)]. Only in the case of the "light, +ΔpH" sample, the ATPase was activated by preillumination for 3 min at 360 μmol m^{-2} s^{-1} in the presence of 0.3 mM ATP. The end of preillumination is denoted by the arrow. As a result, a proton gradient from ATP hydrolysis was maintained after the ATPase activating light was switched off. In the "light, +ΔpH" sample, the maximum fluorescence yield was detected by three saturating pulses during the first 3 min. Thereafter, DCMU (10 μM) and hydroxylammonium chloride (1 mM) were added to keep PS II permanently closed (F_m state) by only the weak modulated measuring beam. For the other two samples, DCMU and hydroxylammonium chloride were added immediately after one saturating pulse.

("light, +ΔpH") is supposed to represent the closed PS II in the dissipative state in leaves as induced by the proton gradient established in strong light. The slight increase in the maximum fluorescence yield occurring during the time course of the measurement is due to some loss in the ΔpH probably caused by the dark inactivation of part of the ATPases. This can be concluded from the time course of the ΔpH-dependent quenching of 9-aminoacridine fluorescence (data not shown; see ref *25*).

After the first saturating flash, DCMU (10 μM) and $HONH_3Cl$ (1 mM) were added to the "reference" and "light, −ΔpH" samples to keep PS II permanently closed by the weak measuring beam. This was done to allow for a better comparison of the results of fluorescence induction and fluorescence decay measurements. Note, however, that both reagents were added to the "light, +ΔpH" sample only after the ATPase had been activated by illumination for 3 min at 360 μmol m^{-2} s^{-1} with the F_m monitored by saturating pulses until the addition.

The photochemical activity of the isolated thylakoids was determined as the level of light-saturated oxygen evolution during electron transport from water to ferricyanide in the presence of 5 mM ammonium chloride as an uncoupler. There were only small losses with a remaining activity of 95% in "light, −ΔpH" samples compared to the reference (not shown). The strong light treatment caused a conversion of violaxanthin to antheraxanthin and zeaxanthin as shown in Table 1.

Table 1: Xanthophyll Cycle Composition in Pea Thylakoids Prepared from Moderately Photoinhibited Leaves[a]

sample	violaxanthin	antheraxanthin	zeaxanthin
"reference"	96	4	nd[b]
"light, −ΔpH"	43	11	46
"light, +ΔpH"	43	11	46

[a] Xanthophyll contents are given as a percentage of the total xanthophyll cycle pool. "Reference", thylakoids prepared from dark-adapted leaves. "Light, −ΔpH", thylakoids prepared from moderately photoinhibited leaves (20 min, 750 μmol m^{-2} s^{-1}). "Light, +ΔpH", thylakoids from moderately photoinhibited leaves; determination of pigments after the sample has passed one complete single-photon timing measurement, including light activation of the ATPase and the subsequent dark incubation in the presence of a proton gradient from ATP hydrolysis. [b] Not detectable.

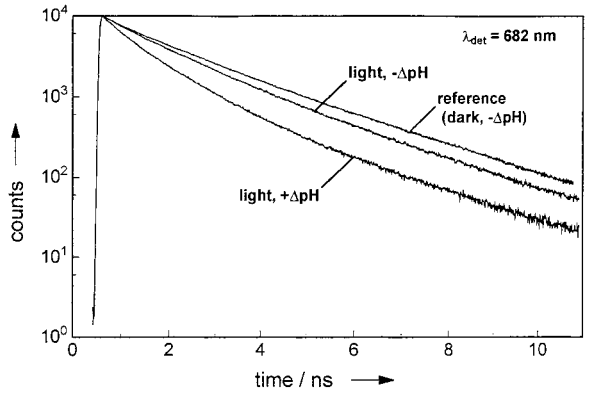

FIGURE 4: Comparison of fluorescence decay kinetics of isolated pea thylakoids in the F_m state. Thylakoids prepared from dark-adapted pea leaves were used as a reference. "Light, −ΔpH" and "light, +ΔpH" samples were prepared from moderately photoinhibited leaves (20 min, 750 μmol m^{-2} s^{-1}). Only in the case of the "light, +ΔpH" sample was a proton gradient from ATP hydrolysis throughout the data collection interval of 10 min. The fluorescence was excited at 643 nm and detected at 682 nm. For each decay curve, a minimum of 23 000 counts were collected in the peak channel of the multichannel analyzer. The chlorophyll content was 10 mg/L. The corresponding maximal steady-state fluorescence yields compared to the reference were 80 and 45% in the "light, −ΔpH" and "light, +ΔpH" samples, respectively. The xanthophyll cycle composition of the different samples is given in Table 1.

Fluorescence Decays with Closed PS II. In Figure 4, the fluorescence decay kinetics of isolated thylakoids with closed PS II at a detection wavelength of 682 nm are depicted for the different samples. Only decays for closed PS II are presented here, because the lack of any substantial difference in the fluorescence yields of open PS II between the different measurement conditions made any further data analysis not promising. Thylakoids were prepared from dark-adapted or moderately photoinhibited leaves. In the case of thylakoids from dark-adapted leaves ("reference" sample) and the nonenergized thylakoids from moderately photoinhibited leaves ("light, −ΔpH" sample), the minimum number of counts for the decay curves was collected in continuous SPT measurements of 50 min. If the measurement condition involved the activity of the ATPase in building up a ΔpH ("light, +ΔpH" sample), the depicted signal represents the sum of counts collected during five independent sampling periods of 10 min each using a fresh sample. In comparison to the reference, the nonenergized thylakoids from moderately photoinhibited leaves ("light, −ΔpH" sample) exhibited accelerated fluorescence decay kinetics (Figure 4) which corresponded to the constant loss in the maximal fluorescence yield observed during steady-state fluorescence measurements. The decay was further accelerated when the membranes were energized by a pH gradient from ATP hydrolysis ("light, +ΔpH" sample).

Global Lifetime Analysis. Similar to what was found by Roelofs et al. (*23*) and Wagner et al. (*5*), the global lifetime data analysis revealed that the fluorescence decays of the three different samples needed to be fitted by a minimum of five exponentials. The resulting decay associated spectra (DAS) are shown in panels a−c of Figure 5. From their spectral characteristics, the two shortest lifetimes of the reference sample (Figure 5a) were attributed to PS I (130 ps) and energy equilibration processes in the light-harvesting antenna complexes of PS II and PS I (40 ps), respectively. Three further components with lifetimes of around 350, 1490, and 2540 ps could be assigned to PS II because of their peaks near 683 nm. Since the main changes in the DAS due to a moderate photoinhibitory pretreatment and the additional presence of a ΔpH were associated with these three PS II lifetimes, we will focus below on these components. Because of changes in their lifetimes that are dependent on the different measurement conditions, we will herein refer to the three PS II components as the slow, the medium, and the fast PS II component, to allow for an easier comparison of the DAS of the different samples.

The DAS of the reference was dominated by the medium PS II component followed by the slow component, while only minor contributions were derived from the fast component (Figure 5a). With only little changes in the three PS II lifetimes, the fluorescence quenching associated with the moderate photoinhibitory treatment ("light, −ΔpH" sample) was mainly caused by a drastic decrease in the relative amplitude of the slow PS II component (Figure 5b). The presence of a ΔpH from ATP hydrolysis ("light, +ΔpH" samples) led to a decrease in the lifetime of the medium component from 1465 to 1178 ps. The fast PS II component exhibited an increase in its relative amplitude and in addition an increase in its lifetime from 376 to 476 ps (Figure 5c). The slow PS II component did not significantly change in response to the additional proton gradient beyond the alterations already seen in the "light, −ΔpH" sample. The PS I component and the component attributed to energy equilibration in the antenna exhibited only minor changes in the different samples.

The conclusions that can be drawn from global lifetime analysis of the chlorophyll fluorescence decay data are limited due to the fact that the determined PS II lifetimes cannot be directly assigned to any specific process within PS II.

Target Analysis. To gain deeper insight into the processes that led to the above-described strong light-induced and ΔpH-dependent changes in fluorescence amplitudes and lifetimes, a target analysis of the fluorescence decay data was necessary. In this target analysis, a heterogeneous exciton/radical pair equilibrium model (see Figure 1) was fitted to the fluorescence decay data, as discussed in detail in ref *23*. The model predicts biexponential fluorescence decay kinetics for PS II subpopulations α and β which are both characterized by their own sets of rate constants and amplitude factors which are proportional to the number of chlorophyll mol-

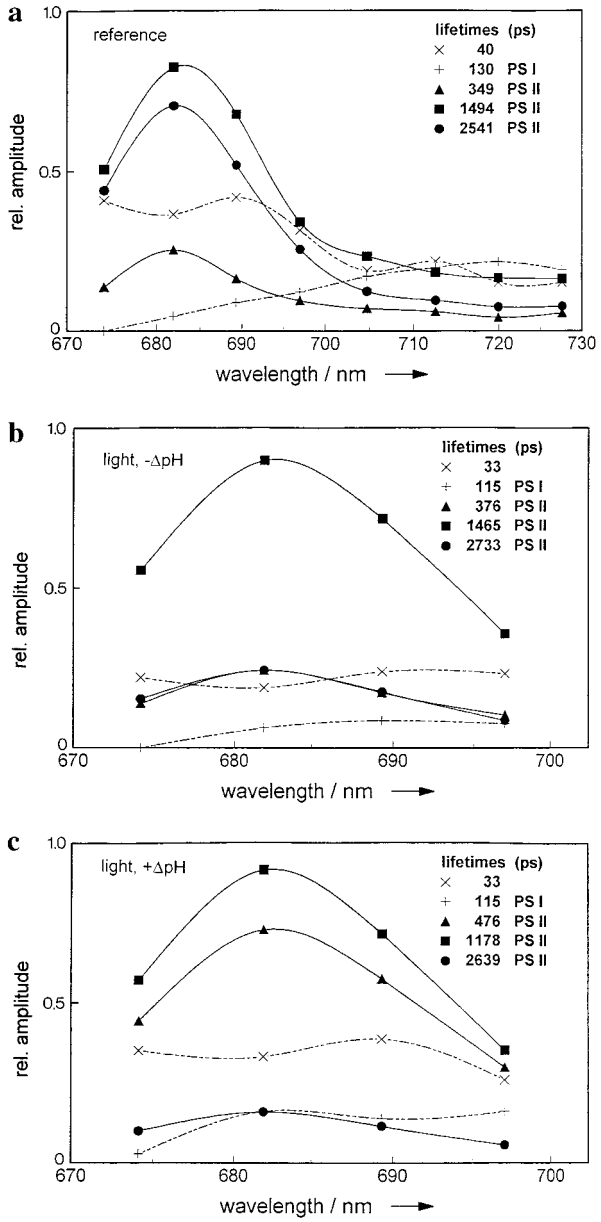

FIGURE 5: Decay-associated spectra (DAS) for isolated pea thylakoids in the F_m state resulting from global lifetime analysis. The excitation wavelength was 643 nm. (a) Reference, nonenergized thylakoids prepared from dark-adapted pea leaves containing no zeaxanthin ($\chi^2 = 1.18$). (b and c) Thylakoids prepared from moderately photoinhibited pea leaves (20 min, 750 μmol m^{-2} s^{-1}) with high contents of zeaxanthin as given Table 1. (b) "Light, $-\Delta$pH" sample, with no further treatment ($\chi^2 = 1.11$). (c) "Light, $+\Delta$pH" sample, where the ATPase was activated by a short light treatment (3 min, 360 μmol m^{-2} s^{-1}) prior to the single-photon timing to establish a proton gradient from ATP hydrolysis during data collection ($\chi^2 = 1.08$). The error range of the lifetimes is 15%. Note that a comparison of relative amplitudes is only valid between particular lifetime components of the same DAS, but not between lifetime components of different DAS.

ecules associated which each type of PS II. In addition to the four resulting lifetimes, two more exponential decay components had to be fitted to the decay data to account for the two lifetimes that could not be attributed to PS II by the global lifetime analysis. This led to a total number of six lifetimes for the thylakoids with closed PS II. We chose to concentrate on the presentation and discussion of the data related to PS II α because of the following considerations.

Table 2: Rate Constants of the Primary Reactions within the Closed PS II According to the Exciton/Radical Pair Equilibrium Model Shown in Figure 1[a]

sample	k_A	k_1	k_{-1}	k_2
"reference" ($k_A = 0.3$ ns^{-1})	0.3	0.4	0.2	1.1
"light, $-\Delta$pH" ($k_A = 0.3$ ns^{-1})	0.3	0.5	0.1	1.8
"light, $-\Delta$pH" ($k_1 = 0.4$ ns^{-1})	0.4	0.4	0.3	1.7
"light, $+\Delta$pH" ($k_A = 0.3$ ns^{-1})	0.3	0.7	0.1	1.2
"light, $+\Delta$pH" ($k_1 = 0.4$ ns^{-1})	0.6	0.4	0.1	1.6

[a] The rate constants k_i (ns^{-1}) were calculated by target analysis of the chlorophyll fluorescence decay kinetics of the different thylakoid samples. Single-photon timing was performed with thylakoids prepared from either dark-adapted ("reference" sample) or moderately photoinhibited pea leaves ("light, $-\Delta$pH" and "light, $+\Delta$pH" samples). In the case of the "light, $+\Delta$pH" sample, a proton gradient from ATP hydrolysis was present throughout the sampling period of 10 min. During data collection, PS II was kept in the closed state by the presence of DCMU (10 μM) and hydroxylammonium chloride (1 mM) in all samples. Although the target analysis was performed for both PS IIα and PS IIβ, only the results for PS IIα are depicted for reasons given in the text. For "light, $-\Delta$pH" and "light, $+\Delta$pH" samples, the target analysis was performed independently with a fixed rate constant of either k_A or k_1. The composition of the xanthophyll cycle in the different samples is given in Table 1. The error ranges of the respective rate constants were as follows: k_A, 25%; k_1, 25%; k_{-1}, 50%; and k_2, 30%.

Among PS II subpopulations, PS II α represents the most functional state with regard to photochemical activity. It binds the majority of the chlorophyll molecules (*19*) and is thus the main origin of chlorophyll fluorescence. Although the rate constants determined for PS II β of the reference sample were similar to the ones found in an earlier study with pea thylakoids (*23*), the changes in the rate constants of PS II β associated with the moderate photoinhibitory pretreatment and the additional presence of a proton gradient fell, however, within relatively large error ranges. Consequently, we felt that any interpretation of these data was not justified.

Unique solutions for the set of differential equations of the exciton/radical pair equilibrium model require one of the four rate constants to be fixed (*18*). The accepted procedure for overcoming this problem was to perform target analysis with a fixed rate constant k_A. This usually well-justified practice is based on the assumption that the probabilities for fluorescent and thermal decay of excited antenna states as well as energy transfer to the reaction center are independent of the reaction center state. However, this presumption cannot be taken for granted in the case of samples with high zeaxanthin content as the latter is expected to excert a direct influence on thermal energy dissipation in the antenna, thus leading to changes in rate constant k_A. We therefore decided to perform target analysis for the zeaxanthin-containing samples independently with a (i) fixed and (ii) variable rate constant k_A.

Assumption I: k_A Is Constant. In a first analysis, the values for rate constants k_1, k_{-1}, and k_2 were calculated with rate constant k_A fixed at 0.3 ns^{-1} for the three different samples. This assumption is derived from earlier observations of average fluorescence lifetimes for the isolated LHC II between 3 and 5 ns (*26*, *27*) and has proven to be a good choice in the case of nonenergized isolated pea thylakoids (*23*). The calculated values for the rate constants are given in Table 2. For the reference sample, the rate contants are in good accord with earlier results (*23*). The sustained fluorescence quenching in thylakoids prepared from strong

light-pretreated leaves ("light, −ΔpH" sample) is mainly due to an increase in rate constant k_2 from 1.1 to 1.8 ns^{-1}, while only small changes were obtained for rate constants k_1 and k_{-1}. With the additional presence of a proton gradient formed by ATP hydrolysis in the thylakoids from moderately photoinhibited leaves ("light, +ΔpH" sample), the situation changed completely in that the former increase in rate constant k_2 was replaced by a near doubling of the rate constant of primary charge separation (k_1). With the high zeaxanthin content of the samples in mind, this result does not easily fit into our present understanding of the role of zeaxanthin in the process of non-photochemical quenching and its dependence on the proton gradient. There is presently no evidence favoring a stimulation of primary charge separation under the combined influences of zeaxanthin and a pH gradient. Therefore, another analysis was performed with a fixed rate constant k_1.

Assumption II: k_1 Is Constant. In a second analysis, rate constant k_1 was fixed at the value of the reference sample (0.4 ns^{-1}). Under this assumption, the main change found in thylakoids from moderately photoinhibited leaves ("light, −ΔpH" sample) was an increase in the rate constant k_2 from 1.1 to 1.7 ns^{-1}. This result is remarkably similar to the one obtained with the first assumption of a fixed rate constant k_A, strongly suggesting that the stable fluorescence quenching induced by the strong light is in fact caused by enhanced radiationless recombination to the ground state and/or triplet excited state of the radical pair. In addition, we also found minor, and perhaps not significant, increases in rate constants k_A and k_{-1}. If a proton gradient from ATP hydrolysis was established across the thylakoids from the moderately photoinhibited leaves ("light, +ΔpH" sample), the rate constant k_2 remained high (1.6 ns^{-1}), but in addition, rate constant k_A was now doubled compared to the reference value (Table 2). The latter result agrees well with our earlier finding that zeaxanthin and the pH gradient cooperate in the induction of antenna quenching as expressed by the enhanced rate constant k_A (*5*). The decision about which of the two above assumptions (a fixed rate constant k_A or k_1) was accurate could not be made by judging only the respective fit quality, because it was essentially equal in both cases. This situation is inherent to the fitted kinetic model shown in Figure 1 in which increases in rate constants k_A and k_1 can, over a wide range, compensate for each other in explaining one and the same acceleration of fluorescence decay kinetics. However, taking into account the additional information that within PS II the xanthophyll cycle carotenoids are at least for the most part bound to the minor LHC II complexes (*29*−*31*), we strongly favor assumption II (fixed k_1). With regard to the unexpected increase calculated for rate constant k_1 in response to a pH gradient in zeaxanthin-containing thylakoids under the assumption of a fixed rate constant k_A, the most reasonable explanation is that the increase in k_1 was only enforced by fixing k_A, thus hiding the true changes in k_2 and k_A.

An important result is that we did not see an influence of the proton gradient on the rate constant for nonradiative recombination to the ground state and/or triplet excited state of the primary radical pair (k_2) in thylakoids from moderately photoinhibited leaves. This would have been predicted from results of a preceding study with dark-adapted isolated thylakoids (*5*).

DISCUSSION

The results of chlorophyll fluorescence induction measurements reveal that a moderate photoinhibitory treatment of pea leaves induced large non-photochemical fluorescence quenching (NPQ). According to the kinetics of dark relaxation, the NPQ was composed of fast reversible qE quenching and slow reversible qI quenching. The qI in photoinhibited leaves must be considered independent of the proton gradient since the qI was also found in thylakoids which were prepared from those leaves and then stored in the dark. In these thylakoids, qE quenching could be regenerated in the dark using a proton gradient driven by ATP hydrolysis.

Using thylakoid samples which were treated in the same manner as in the steady-state fluorescence measurements, qI and qE were further studied by combined global and target analysis of the respective chlorophyll fluorescence decays. According to global lifetime analysis, the qI quenching ("light, −ΔpH" sample) was mainly characterized by a decrease in the relative amplitude of the longest-lived PS II fluorescence decay component ($\tau = 2730$ ps). In this respect, the qI quenching induced by strong light resembles a particular component of qE which has recently been shown to be connected to a proton gradient in thylakoids from dark-adapted leaves (*5*). With regard to global lifetime analysis, this formerly observed qE type and the qI quenching investigated in the study presented here are both characterized mainly by significant decreases in comparatively slow PS II lifetimes of 2800 and 2730 ps, respectively. These results provide first evidence for similarities in the mechanisms of the two types of quenching.

In comparison to the reference, the "light, +ΔpH" sample of this study, in which fluorescence was simultaneously quenched by qE and qI, was characterized by a decrease in the relative amplitude of the longest-lived PS II component (2640 ps) along with an increase in the amplitude of the fast component (476 ps). In addition, the lifetime of the medium PS II component (1180 ps) decreased compared to that of the reference (1490 ps). Under the assumption that the amplitude decrease in the slow PS II component was still attributed to qI, the qE by itself would then be related to the relative amplitude increase of the fast component and the lifetime decrease in the medium PS II component. In a previous study (*5*), where thylakoids from dark-adapted pea leaves were used, we have demonstrated that a ΔpH from ATP hydrolysis may drive zeaxanthin synthesis, and that the combined effect of the ΔpH and zeaxanthin was qE quenching which was also associated with both an amplitude increase of a fast PS II component (525 ps) and a lifetime decrease in a medium PS II component (1224 ps) compared to that of the respective reference (1416 ps). We thus conclude that the qE observed in this study can also be explained by the presence of both zeaxanthin and a ΔpH. However, our results from global lifetime analysis do not exclude the alternative explanation that the qI, and not the qE, was related to zeaxanthin and the qE was exclusively associated with the ΔpH. We shall refer to this point in the discussion of the target analysis.

The qI from moderate in vivo light treatment corresponded to a decreased amplitude of a particular PS II lifetime with only minor changes in the lifetime itself. In con-

trast to our findings, it has been reported by Gilmore and co-workers (*28*) that a larger qI due to a stronger in vitro light treatment was associated with a gradual shift of a 1.9 ns lifetime component with constant amplitude toward shorter lifetimes. These differing results may possibly be explained in terms of primary and advanced stages of photoinhibition in the two studies and different photoinhibitory and analytical procedures that were applied. Interestingly, the two fluorescence lifetime studies revealed similar results regarding qE, which was associated with an increase in the relative amplitude of a lifetime arround 500 ps in both cases.

While the global lifetime analysis approach did only allow the mere distinction between qE and qI in terms of changes in lifetimes and amplitudes, it was the strength of target analysis that it not only facilitated the assignment of the two types of quenching to defined events within PS II but also allowed their quantitative estimation during their simultaneous operation.

According to the target analysis based on the heterogeneous exciton/radical pair equilibrium model shown in Figure 1, the qI is best explained by an increase in the level of nonradiative recombination of the charge-separated state back to the ground state and/or to the triplet excited state as indicated by the enhanced rate constant k_2. The additional qE quenching induced by the ΔpH is related to an increase in rate constant k_A, which indicates enhanced thermal dissipation in the PS II antenna. It is thus possible to make a clear distinction between qI and qE in that the first is pure reaction center quenching while the second is antenna quenching. The clear assignment of zeaxanthin to either qE or qI is difficult because zeaxanthin was present during the measurement of both types of quenching. Two alternative assignments are considered.

(i) Zeaxanthin Is Related to qI. A stimulation of nonradiative recombination of the primary radical pair ($P\text{-}680^+$ $Pheo^-$) by zeaxanthin requires interaction between zeaxanthin and the primary radical pair. Since it is widely accepted that zeaxanthin is restricted to the outer PS II antenna (*29*−*31*), such an interaction may be excluded. Nevertheless, if such an interaction is assumed, the observed antenna quenching would then exclusively be related to the ΔpH. As a consequence, the established role of zeaxanthin in antenna quenching would have to be questioned. In our study, the qI was not antenna quenching, thus ruling out sustained quenching by antenna-localized zeaxanthin. Apart from these considerations, our results do not exclude a possible role of zeaxanthin in sustained quenching during stronger photoinhibitory treatment (*11*, *12*, *32*). In this case of antenna-localized qI, the relation between sustained F_o quenching and long-lived amounts of zeaxanthin must be established in accordance with currently accepted PS II models.

(ii) Zeaxanthin Is Related to qE. Since in this study the target analysis led to an assignment of qE to the PS II antenna, the assumption that zeaxanthin is related to qE is consistent with the present knowledge regarding the localization of zeaxanthin. It is at first glance inconsistent with the fact that despite high zeaxanthin contents we did not observe any antenna quenching in samples without a proton gradient. On the other hand, it has been shown previously that in isolated thylakoids zeaxanthin-dependent quenching ceased immediatly upon uncoupling (*5*). Our results are therefore consistent with the view that besides its role in zeaxanthin synthesis the ΔpH could have a second important role in zeaxanthin-dependent antenna quenching. It was suggested that unlike in solution, where the S_1 energy of zeaxanthin seems sufficiently low for direct quenching of Chl *a* S_1 states (*33*), the quenching capability of zeaxanthin in a native system might depend on the proton gradient in a dual manner (*34*). (i) The ΔpH might induce asymmetric perturbations in the vicinity of the membrane-spanning molecule zeaxanthin which could then increase the dipole strength of the formally dipole-forbidden zeaxanthin S_1 to S_0 transition. (ii) ΔpH responsive changes in the S_1 energy of Chl *a* might increase its level of spectral overlap with the zeaxanthin S_1 state (*34*). Note, however, the recent finding of a role in light harvesting of zeaxanthin in a zeaxanthin epoxidase mutant of *Arabidopsis thaliana* where zeaxanthin and lutein are the only carotenoids in LHC II (*35*).

The above assumption, that zeaxanthin can be attributed to qE, is also supported by the results of global lifetime analysis of qE quenching which strongly resemble those of zeaxanthin- and ΔpH-dependent qE in thylakoids from dark-adapted leaves (*5*). It is therefore preferred to the alternative assumption which relates it to qI.

With regard to the dependence of antenna quenching on zeaxanthin and ΔpH, our data are also consistent with suggestions by Horton and Ruban (*36*) who discussed the possibility of ΔpH-dependent zeaxanthin aggregation, which might then enable a quenching mechanism based on the formation of exciton-coupled Chl *a* dimers as suggested by Crofts and Yerkes (*37*).

The mechanism behind the stimulation of nonradiative charge recombination remains unknown. If a partial loss of PS II donor side activity was assumed, it could at first glance be related to the enhanced stability of the quenching species $P\text{-}680^+$ (*38*). However, the described method of single-photon timing together with the use of a flow cuvette in our study should have eliminated the possibility of excitation of the oxidized primary donor ($P\text{-}680^+$). Preferential charge recombination may be linked to the earlier reported primary photoinhibitory loss in normal secondary electron transfer between Q_A and Q_B (*39*−*41*) by one and the same structural change.

Apart from considerations regarding the mechanism of qI quenching, this study provides evidence for a close relation between qI and a particular qE component existing in thylakoids from dark-adapted leaves (*5*, *6*). Target analysis indicates that this qE component as well as the qI observed in this study is related to enhanced nonradiative charge recombination; thus, both represent reaction center quenching. As outlied above, global lifetime analysis further demonstrates that they are both characterized by a decrease in their longest-lived PS II lifetime component. The two types of reaction center quenchings differ only with respect to the role of the proton gradient. We therefore propose that during strong light exposure a ΔpH-dependent reaction center qE component is replaced by a reaction center qI. In agreement with earlier suggestions (*8*, *42*), the qI would then represent stable downregulation of PS II rather than damage. The enhanced nonradiative charge recombination may provide a mechanism for the harmless deactivation of potentially damaging radical pair states. This interpretation is in line

with earlier conclusions by Roelofs et al. (*23*) about the photoprotective nature of the increased level of nonradiative charge recombination in the closed PS II in comparison to that in the open PS II.

REFERENCES

1. Demmig, B., and Winter, K. (1988) *Aust. J. Plant Physiol. 15*, 163−178.
2. Krause, G. H., and Weis, E. (1991) *Annu. Rev. Plant Physiol. Plant Mol. Biol. 42*, 313−349.
3. Briantais, J.-M., Vernotte, C., Picaud, M., and Krause, G. H (1979) *Biochim. Biophys. Acta 548*, 128−138.
4. Demmig-Adams, B., Adams, W. W., Heber, U., Neimanis, S., Winter, K., Krüger, A., Czygan, F.-C., Bilger, W., and Björkman, O. (1990) *Plant Physiol. 92*, 293−301.
5. Wagner, B., Goss, R., Richter, M., and Holzwarth, A. R. (1996) *J. Photochem. Photobiol., B 36*, 339−350.
6. Goss, R., Richter, M., Wagner, B., and Holzwarth, A. (1995) in *Photosynthesis: from Light to Biosphere* (Mathis, P., Ed.) Vol. IV, pp 87−90, Kluwer Academic Publishers, Dordrecht, The Netherlands.
7. Krause, G. H (1988) *Physiol. Plant. 74*, 566−574.
8. Öquist, G., Chow, W. S., and Anderson, J. M. (1992) *Planta 186*, 450−460.
9. Cleland, R. E., Melis, A., and Neale, P. J. (1986) *Photosynth. Res. 9*, 79−88.
10. Demmig-Adams, B., Winter, K., Krüger, A., and Czygan, F.-C. (1989) *Plant Physiol. 90*, 887−893.
11. Thiele, A., Schirwitz, K., Winter, K., and Krause, G. H. (1996) *Plant Sci. 115*, 237−250.
12. Jahns, P., and Miehe, B. (1996) *Planta 198*, 202−210.
13. Ruban, A. V., and Horton, P. (1995) *Plant Phys. 108*, 721−726.
14. Gilmore, A. M., and Björkman, O. (1994) *Planta 192*, 526−536.
15. Schatz, G. H., Brock, H., and Holzwarth, A. R. (1988) *Biophys. J. 54*, 397−405.
16. Chow, W. S., and Anderson, J. M. (1987) *Aust. J. Plant Physiol. 14*, 1−8.
17. Holzwarth, A. R., Schatz, G. H., Brock, H., and Colombano, C. G. (1988) Picosecond Phenomena VI, *Springer Ser. Chem. Phys. 48*, 602−605.
18. Roelofs, T. A., and Holzwarth, A. R. (1990) *Biophys. J. 57*, 1141−1153.
19. Melis, A. (1991) *Biochim. Biophys. Acta 1058*, 87−106.
20. Melis, A., and Anderson, J. M. (1983) *Biochim. Biophys. Acta 724*, 473−484.
21. Bassi, R., Marquardt, J., and Lavergne, J. (1995) *Eur. J. Biochem. 233*, 709−719.
22. Andersson, B., and Anderson, J. M. (1980) *Biochim. Biophys. Acta 593*, 427−440.
23. Roelofs, T. A., Lee, C.-H., and Holzwarth, A. R. (1992) *Biophys. J. 61*, 1147−1163.
24. Aro, E.-M., Virgin, I., and Andersson, B. (1993) *Biochim. Biophys. Acta 1142*, 113−134.
25. Schuldiner, S., Rottenberg, H., and Avron, M. (1972) *Eur. J. Biochem. 25*, 64−70.
26. Lotshaw, W. T., Alberte, R. S., and Fleming, G. R. (1982) *Biochim. Biophys. Acta 682*, 75−85.
27. Hodges, M., Moya, J.-M., and Remy, R. (1987) in *Progress in Photosynthesis Research* (Biggins, J., Ed.) Vol. 86, pp 115−118, Nijhoff, Dordrecht, The Netherlands.
28. Gilmore, A. M., Hazlett, T. L., Debrunner, P. G., and Govindjee (1996) *Photochem. Photobiol. 64*, 552−563.
29. Bassi, R., Pineau, B., Dainese, P., and Marquardt, J. (1993) *Eur. J. Biochem. 212*, 297−303.
30. Ruban, A. V., Young, A. J., Pascal, A. A., and Horton, P. (1994) *Plant Physiol. 104*, 227−234.
31. Goss, R., Richter, M., and Wild, A. (1997) *J. Plant Physiol. 151*, 115−119.
32. Adams, W. W., and Demmig-Adams, B. (1995) *Plant Cell Environ. 18*, 117−127.
33. Frank, H. A., Chynwat, V., Young, A., Gosztola, D., and Wasiliewsky, M. R. (1994) *Photosynth. Res. 41*, 389−395.
34. Owens, T. G. (1994) in *Photoinhibition of Photosynthesis. From Molecular Mechanisms to the Field* (Baker, N. R., and Bowyer, J. R., Eds.) pp 95−110, Bios Scientific Publishers, Oxford, U.K.
35. Connelly, J. P., Müller, M. G., Bassi, R., Croce, R., and Holzwarth, A. R. (1997) *Biochemistry 36*, 281−287.
36. Horton, P., and Ruban, A. V. (1994) in *Photoinhibition of Photosynthesis. From Molecular Mechanisms to the Field* (Baker, N. R., and Bowyer, J. R., Eds.) pp 111−128, Bios Scientific Publishers, Oxford, U.K.
37. Crofts, A. R., and Yerkes, C. T. (1994) *FEBS Lett. 352*, 265−270.
38. Bruce, D., Samson, G., and Carpenter, C. (1997) *Biochemistry 36*, 749−755.
39. Ohad, I., Koike, H., Shochat, S., and Inoue, Y. (1988) *Biochim. Biophys. Acta 933*, 288−298.
40. Richter, M., Rühle, W., and Wild, A. (1990) *Photosynth. Res. 24*, 229−235.
41. Briantais, J.-M., Ducruet, J.-M., Hodges, M., and Krause, G. H. (1992) *Photosynth. Res. 31*, 1−10.
42. Anderson, J. M., Chow, W. S., and Öquist, G. (1993) in *Current Topics in Plant Physiology Volume 8, Photosynthetic Responses to the Environment* (Yamamoto, H. Y., and Smith, C. M., Eds.) pp 14−26, American Society of Plant Physiologists, Rockville. MD.

BI983009A